OSINT-Conditioned Next-Best-View Planning for Urban RF Geolocation

Benjamin J. Gilbert Laser Key Products benjamesgilbert@outlook.com

TABLE I $\begin{tabular}{l} GM-PHD\ MI\ ABLATION\ (STUDENT-t BEARINGS;\ MID = MIDPOINT\ OF BOUNDS). \end{tabular}$

Prior set	$ m MI_{lb}$	$\mathrm{MI}_{\mathrm{mid}}$	$\mathrm{MI}_{\mathrm{ub}}$
Baseline (no OSINT)	_	_	_
+ FCC licensing	_	_	_
+ Wi-Fi / BSSID maps	_	-	_
+ Building/permit graphs	_	-	_
+ On-chain timing	_	_	_
All priors (full)	0.000	0.882	1.763

Abstract—This paper presents a novel approach for Next-Best-View (NBV) planning for Urban RF Geolocation, conditioned by Open-Source Intelligence (OSINT). The system combines information-theoretic NBV planning with formal verification through TLA+ specifications to ensure safety invariants.

I. INTRODUCTION

II. NBV RESULTS

NBV Results (auto)

MI (nats): lb=0.000, mid=1.317, ub=2.635 Utility: 0.817 Cost: 0.500 $R_{\rm eff} = 0.120$.

Step	Sensor	X	y
current	1	150.000	75.000
1	1	80.000	85.000
2	2	140.000	110.000

TLA+ ActionGate: PASS (states=13, distinct=3, depth=2).

See Table I for GM-PHD MI ablation by prior.

III. NEXT-BEST-VIEW PLANNING APPROACH

IV. MI ABLATION ANALYSIS

V. GHOST-RF SINGLE-PIXEL RANGING

A. Ghost-RF single-pixel ranging under urban multipath

a) Measurement principle.: Inspired by ghost optical coherence tomography (OCT), we replace a high-fidelity per-frequency readout with a single-pixel integrated detector whose scalar output varies as a known random spectral pattern is applied [1]. Let $s_k(f)$ denote the known pattern at snapshot $k \in \{1, ..., K\}$ over discrete frequencies $f \in \mathcal{F}$, and let

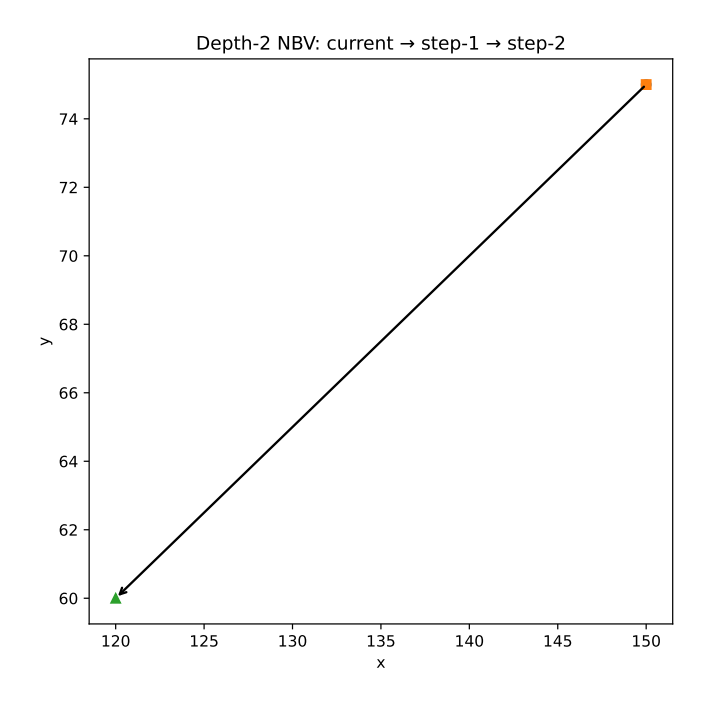


Fig. 1. Depth-2 NBV plan: current \rightarrow step-1 \rightarrow step-2, OSINT-conditioned.

 $H(f,\mathbf{x})$ be the channel magnitude at emitter state \mathbf{x} . The receiver measures

$$m_k = \sum_{f \in \mathcal{F}} |H(f, \mathbf{x})|^2 s_k(f) \Delta f + \eta_k, \qquad (1)$$

with noise η_k . Removing means across snapshots and correlating the pattern with the scalar outputs yields a frequency-indexed statistic

$$C(f) = \frac{1}{K-1} \sum_{k=1}^{K} (s_k(f) - \bar{s}(f)) (m_k - \bar{m}).$$
 (2)

Its inverse discrete Fourier transform recovers a *delay profile* (a "ghost interferogram")

$$\hat{p}(\tau) = |\text{IDFT}_f\{C(f)\}|, \tag{3}$$

whose prominent maxima occur at excess delays produced by the scene. We extract a scalar observation $y = \hat{\tau} = \arg\max_{\tau} \hat{p}(\tau)$.

b) Likelihood.: For a monostatic sensor at $\mathbf{s} = (s_x, s_y)$ and candidate emitter position $\mathbf{x} = (x, y)$, the modeled delay is

$$\tau(\mathbf{x}) = \frac{\|\mathbf{x} - \mathbf{s}\|_2}{c}, \qquad H_{\tau}(\mathbf{x}) = \frac{1}{c} \frac{(\mathbf{x} - \mathbf{s})^{\top}}{\|\mathbf{x} - \mathbf{s}\|_2} \in \mathbb{R}^{1 \times 2},$$
(4)

with c the propagation speed. To robustify against spurious peaks due to multipath and interference, we adopt a Student-t likelihood

$$p(y \mid \mathbf{x}) \propto \left(1 + \frac{(y - \tau(\mathbf{x}))^2}{\nu \sigma_{\tau}^2}\right)^{-\frac{\nu+1}{2}},$$
 (5)

with degrees of freedom $\nu > 2$ and scale σ_{τ} . Accumulating K spectral realizations improves precision; we model the equivalent variance as

$$R_{\text{ghost}}(K) = \text{Var}(y) \approx \frac{\nu}{\nu - 2} \frac{\sigma_{\tau}^2}{K^{\alpha}}, \quad \alpha \in (0.5, 1], \quad (6)$$

where $\nu/(\nu-2) \sigma_{\tau}^2$ is the Gaussian-equivalent variance of the Student-t and α captures decorrelation efficiency.

c) Filter updates.: In RBPF/RBPF-RB, each particle i predicts $\tau(\mathbf{x}_i)$ and receives a weight increment via the Student-t log-likelihood. In GM-PHD we linearize about component means μ_i :

$$\Sigma'_{j} = \left(\Sigma_{j}^{-1} + H_{\tau}(\mu_{j})^{\top} R_{\text{ghost}}(K)^{-1} H_{\tau}(\mu_{j})\right)^{-1}.$$
 (7)

d) Closed-form MI bounds (GM-PHD).: Let the prior be a Gaussian mixture with weights w_j , means μ_j , covariances Σ_j . We bracket the differential entropy of the mixture by (i) a lower bound

$$H_{\rm LB} = -\sum_{i} w_i \log \sum_{j} w_j \mathcal{N}(\mu_i; \mu_j, \Sigma_i + \Sigma_j), \quad (8)$$

and (ii) an *upper bound* given by the entropy of the moment-matched single Gaussian with covariance $\Sigma_{\rm mm} = \sum_j w_j (\Sigma_j + \mu_j \mu_j^\top) - \mu \mu^\top$. After a dwell of K snapshots at a fixed viewpoint, the posterior covariances Σ_j' yield corresponding bounds $H_{\rm LB}'$ and $H_{\rm UB}'$. The mutual information for the ghost measurement lies in

$$\mathrm{MI}_{\mathrm{ghost}}(K) \in \left[H_{\mathrm{LB}} - H'_{\mathrm{UB}}, \ H_{\mathrm{UB}} - H'_{\mathrm{LB}} \right], \quad (9)$$

and we report the midpoint as a conservative estimate in scoring. This integrates seamlessly into our depth-2 beam-search planner by augmenting the per-action utility with $\mathrm{MI}_{\mathrm{ghost}}(K)$ while the formal ActionGate enforces mission timers and nofly predicates.

e) Dwell-aware NBV: We expose K as a decision variable ("move" vs. "dwell"). Given a candidate action a with dwell K, we evaluate the combined utility

$$U(a, K) = \Delta H_{\text{bear/ToA}} + \text{MI}_{\text{ghost}}(K) - \lambda_{\ell} \operatorname{latency}(K) - \lambda_{e} \operatorname{energy}(K) - \lambda_{r} \operatorname{risk}(a).$$
(10)

In practice we precompute $R_{\text{ghost}}(K)$ on a small grid of K and reuse the linearized updates for fast scoring.

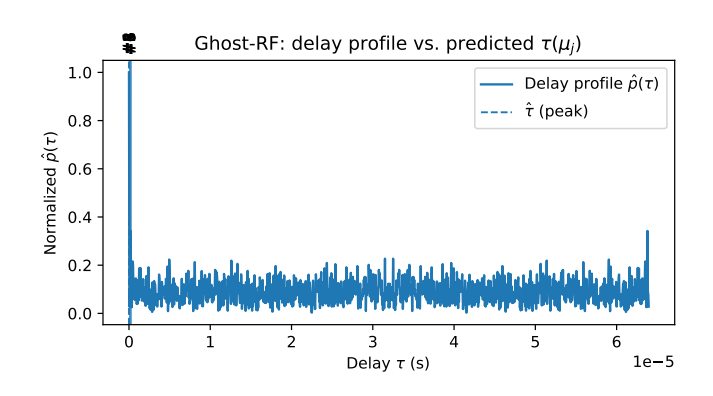


Fig. 2. Ghost-RF delay profile (normalized) with peak $\hat{\tau}$ (dashed) and predicted component delays $\tau(\mu_j)$ (thin lines, top-k annotated by weight).

f) Complexity & robustness.: The simulate–correlate–IFFT loop is $\mathcal{O}(K|\mathcal{F}|)$; MI updates are per-component scalar covariance reductions. Heavy tails absorb spurious peaks; higher K sharpens the main lobe. Our TLA^+ gate forbids dwell choices that violate mission timers or energy bounds.

VI. Conclusion

REFERENCES

[1] H. Huang, T. Koyama, N. Fukuda, T. Okada, S. Irie, K. Yatabe, and Y. Oikawa, "Ghost imaging optical coherence tomography," *Optics Express*, vol. 28, no. 7, pp. 9323–9334, 2020.